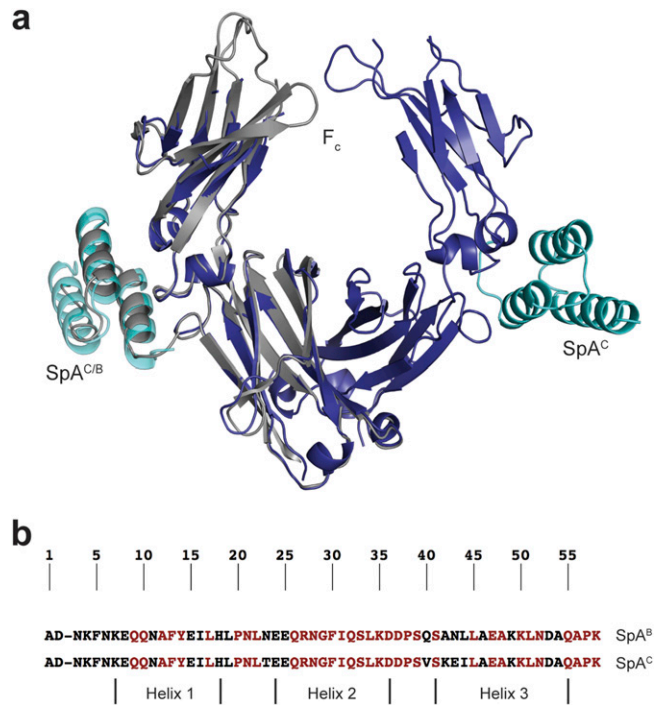
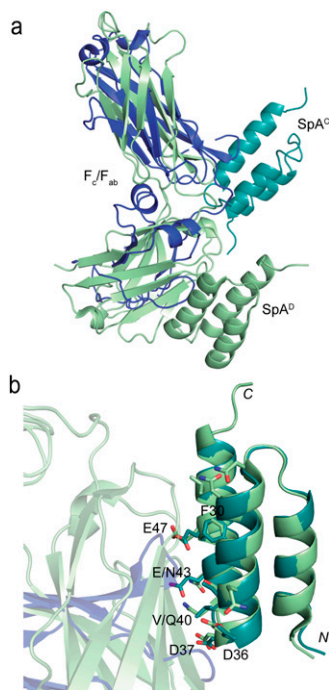


# Supporting Information

Deis et al. 10.1073/pnas.1424724112



**Fig. S1.** Comparison between PDB ID codes 1FC2 and 4WWI, our new  $F_c$ - $SpA^C$  complex structure. (A)  $SpA^B$  in 1FC2 binds to the same site on  $F_c$  as does  $SpA^C$  in the new complex. The  $F_c$  portions of both structures superimpose well. According to ref. 30, helix 3 in 1FC2 was folded irregularly and no density was observed, although nonhelical coordinates were still modeled. (B)  $SpA^B$  and  $SpA^C$  contain minimal sequence differences, none of which are interfacial. Red residues are identical in all five SpA protein binding domains.



**Fig. S2.** SpA<sup>C</sup> and F<sub>c</sub> bind in a secondary mode. (A) SpA<sup>C</sup> (dark cyan) binds to F<sub>c</sub> (blue) in a different location from SpA<sup>D</sup> binding to F<sub>ab</sub> (green; from PDB ID code 1DEE). (B) The helix 2/3-binding sites on the SpA domain are nearly homologous, with only a few rotamer differences.

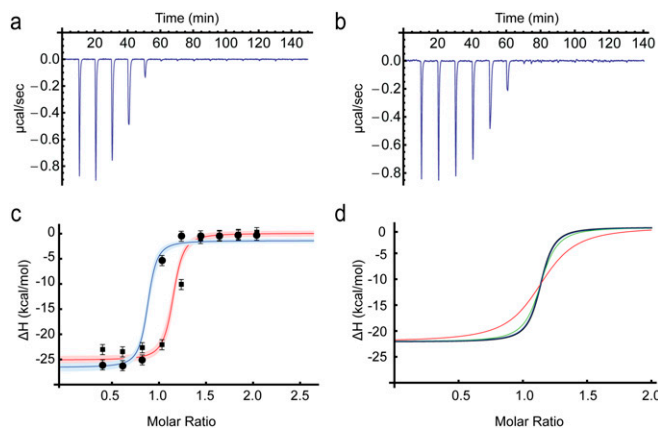


**Fig. S3.** Isothermal titration calorimetry data of SpA<sup>C</sup>-F<sub>c</sub> binding. (A and B) Raw data for (A) titration of 5 μM SpA<sup>C</sup> with F<sub>c</sub> and (B) titration of 5 μM F<sub>c</sub> with SpA<sup>C</sup>. (C) Best-fit ITC binding isotherms for titration of F<sub>c</sub> into SpA<sup>C</sup> (squares, red line) and SpA<sup>C</sup> into F<sub>c</sub> (circles, blue line). Bands represent 95% confidence intervals of best-fit isotherms. Error bars represent SEM. Best-fit parameter values (95% confidence interval) are  $K_a$ ,  $6.6$  ( $5.6, 9.5$ )  $\times 10^7$  M<sup>-1</sup>;  $\Delta H$ ,  $-25.4$  ( $-25.8, -24.6$ ) kcal/mol;  $n = 1.14$  (1.13, 1.15). (D) Binding isotherms for titration of SpA<sup>C</sup> with F<sub>c</sub> were simulated using a two-site-binding model with the affinity, enthalpy, and  $n$  values given in C. Simulated single-site isotherm (black) and simulated two-site isotherms at various second-site  $K_d$  values: 1 μM (red), 10 μM (green), 100 μM (blue).

**Table S1. Data collection and refinement statistics for the SpA<sup>C</sup>-F<sub>c</sub> complex**

	SpA <sup>C</sup> -F <sub>c</sub> complex
<b>Data collection</b>	
Space group	C2
Cell dimensions	
<i>a</i> , <i>b</i> , <i>c</i> , Å	139.0, 88.1, 101.0
α, β, γ, °	90.0, 91.0, 90.0
Wavelength	1.0
Resolution, Å	50.00–2.30 (2.34–2.30)*
<i>R</i> <sub>sym</sub>	0.17 (1.0)
<i>I</i> / <i>σ</i> <i>I</i>	29.0 (1.7)
Completeness, %	99.5 (94.8)
Redundancy	14.8 (12.3)
<b>Refinement</b>	
Resolution, Å	41.18–2.31
No. of reflections	50,556
<i>R</i> <sub>work</sub> / <i>R</i> <sub>free</sub>	21.2/25.0
No. of atoms	
Protein	6254
Water	165
B factors	
Protein	62.96
Water	76.44
Rms deviations	
Bond lengths, Å	0.004
Bond angles, °	0.817

\*Data were collected from a single crystal. Values in parentheses are for the highest-resolution shell.

Table S2.  $R_p$  for apo SpA<sup>C</sup> and SpA<sup>C</sup> in complex with F<sub>c</sub>

Residue	Complex (4VWWI)			Residue	Complex (4VWWI)		
	Apo (4NPD)	chain A	$\frac{R_p^{\text{apo}} - R_p^{\text{cmplx}}}{R_p^{\text{apo}}}, \%$		Apo (4NPD)	chain A	$\frac{R_p^{\text{apo}} - R_p^{\text{cmplx}}}{R_p^{\text{apo}}}, \%$
N3	0.59	0.25	58	F30	1.01	0.20	80
K4	0.88	0.80	9	I31*	0.81	0.26	68
F5	0.98	0.45	55	Q32	0.77	0.30	61
N6	0.98	0.12	88	S33	1.00	0.28	72
K7	0.67	0.58	13	L34	0.59	0.07	88
E8	0.70	0.72	-3	K35	0.58	0.29	50
Q9	0.69	0.12	83	D36	0.47	0.06	87
Q10*	0.74	0.16	78	D37	0.98	0.06	94
N11	0.43	0.91	-112	P38	0.52	0.53	-2
F13*	0.79	0.14	82	S39	0.77	0.44	43
Y14*	0.93	0.01	99	V40	0.78	0.50	36
E15	0.65	0.78	-20	S41	0.85	0.27	68
I16	0.85	0.18	79	K42	0.49	0.60	-22
L17*	0.80	0.02	98	E43	0.72	0.28	61
H18*	0.97	0.11	89	I44	0.79	0.45	43
L19	0.88	0.04	95	L45	0.85	0.38	55
P20	0.75	0.33	56	E47	0.94	0.57	39
N21	0.82	0.08	90	K49	0.84	0.35	58
L22	0.95	0.19	80	K50	0.59	0.50	15
T23	0.95	0.43	55	L51	0.87	0.20	77
E24	0.59	0.50	15	N52	0.94	0.39	59
E25	0.59	0.60	-2	D53	0.68	0.23	66
Q26	1.00	0.16	84	Q55	1.00	0.19	81
R27	0.88	0.36	59	P57	0.84	0.15	82
N28	0.60	0.12	80	K58	0.35	0.47	-34

## Statistics comparing interfacial and noninterfacial residues

Residue type	Apo mean	Complex mean	$\frac{R_p^{\text{apo}} - R_p^{\text{cmplx}}}{R_p^{\text{apo}}}, \%$
All	0.77 (0.17) <sup>†</sup>	0.32 (0.22)	53 (42)
Interfacial	0.84 (0.09)	0.12 (0.09)	86 (12)
Noninterfacial	0.76 (0.18)	0.35 (0.22)	48 (42)

}  $P = 0.00007^{\ddagger}$ 

It is difficult to quantitatively estimate the uncertainty in electron-density values; therefore, we have not included uncertainties in  $R_p$ . Qualitatively, sources of error that contribute to uncertainty in electron density and therefore  $R_p$  include data collection errors, crystal defects, modeling errors, and refinement artifacts.

\*Interfacial residues.

<sup>†</sup>Numbers in parentheses are SDs.

<sup>‡</sup>Based on a Student  $t$  hypothesis test. The  $P$  value is the probability that interfacial and noninterfacial residues have the same reductions in conformational heterogeneity upon F<sub>c</sub> binding.

**Table S3. Comparison of NMR and crystallographic observations of conformational heterogeneity**

Residue	Apo (X-ray)*	Apo (NMR) <sup>†</sup>	<sup>3</sup> J(Hz)	Chemical shift	Complex (X-ray)*	Complex $\rho$ ratio <sup>‡</sup>	Note
K4	$\chi_1$ : +	$\chi_1$ : +	${}^3J(C\gamma C') = 2.72 \pm 0.01$		$\chi_1$ : +	0.57	
K7	$\chi_1$ : +	$\chi_1$ : +	${}^3J(C\gamma C') = 2.61 \pm 0.01$		$\chi_1$ : +	0.45	
I16	$\chi_1$ : -	$\chi_1$ : -	${}^3J(C\gamma_1 C') = 3.95 \pm 0.05$	$C(\delta_1) = 13.7$ ppm	$\chi_1$ : -	0.07	From NMR scalar coupling and chemical shift:
	$\chi_2$ : -	$\chi_2$ : +	${}^3J(C\gamma_1 N) = 0.37 \pm 0.21$ ; ${}^3J(C\gamma_2 C') = 1.09 \pm 0.01$ ; ${}^3J(C\gamma_2 N) = 2.10 \pm 0.01$		$\chi_2$ : -		Population trans 0.80 Population gauche- 0.20
L17 <sup>§</sup>	$\chi_1$ : a	$\chi_1$ : +	${}^3J(C\gamma C') = 2.97 \pm 0.02$	$C(\delta_1) = 24.7$ ppm	$\chi_1$ : -	0.24	
	$\chi_2$ : a	$\chi_2$ : +	${}^3J(C\gamma N) = 0.74 \pm 0.07$	$C(\delta_2) = 23.0$ ppm; $\Delta CS = 1.7$ ppm	$\chi_2$ : -		
L19	$\chi_1$ : -	$\chi_1$ : -	${}^3J(C\gamma C') = 3.80 \pm 0.04$ ;	$C(\delta_1) = 26.6$ ppm	$\chi_1$ : -	0.13	
	$\chi_2$ : a	$\chi_2$ : +	${}^3J(C\gamma N) = 0.73 \pm 0.20$	$C(\delta_2) = 22.8$ ppm; $\Delta CS = 3.8$ ppm			
L22	$\chi_2$ : -	$\chi_2$ : -		$C(\delta_1) = 27.2$ ppm; $C(\delta_2) = 22.2$ ppm; $\Delta CS = 5.0$ ppm	$\chi_2$ : -	0.3	
T23	$\chi_1$ : -	$\chi_1$ : +	${}^3J(C\gamma_2 C') = 3.06 \pm 0.01$ ; ${}^3J(C\gamma_2 N) = 1.08 \pm 0.01$		$\chi_1$ : -	0.1	Crystal contact
I31 <sup>§</sup>	$\chi_1$ : -	$\chi_1$ : -	${}^3J(C\gamma_1 C') = 3.72 \pm 0.03$ ;	$C(\delta_1) = 12.4$ ppm	$\chi_1$ : -	0.13	
L34	$\chi_2$ : m	$\chi_2$ : +	${}^3J(C\gamma_1 N) = 0.36 \pm 0.20$				
		$\chi_2$ : +	$\chi_2$ : +		$C(\delta_1) = 25.5$ ppm; $C(\delta_2) = 25.4$ ppm; $\Delta CS = 0.1$ ppm	$\chi_2$ : +	0.63
V40	$\chi_1$ : -	$\chi_1$ : -	${}^3J(C\gamma_1 C') = 1.05 \pm 0.01$ ; ${}^3J(C\gamma_1 N) = 0.72 \pm 0.01$ ; ${}^3J(C\gamma_2 C') = 3.65 \pm 0.01$ ; ${}^3J(C\gamma_2 N) = 0.45 \pm 0.02$		$\chi_1$ : -	0.10	
I44	$\chi_1$ : -	$\chi_1$ : -	${}^3J(C\gamma_1 C) = 3.60 \pm 0.02$ ;	$C(\delta_1) = 13.0$ ppm	$\chi_1$ : -	0.22	
	$\chi_2$ : a	$\chi_2$ : +	${}^3J(C\gamma_1 N) = 0.52 \pm 0.15$ ; ${}^3J(C\delta_1 C\alpha) = 2.77 \pm 0.01$				
L45	$\chi_1$ : -	$\chi_1$ : ?		$C(\delta_1) = 23.8$ ppm	$\chi_1$ : -	0.26	From NMR chemical shifts:
	$\chi_2$ : -	$\chi_2$ : -		$C(\delta_2) = 24.5$ ppm; $\Delta CS = -0.7$ ppm	$\chi_2$ : -		Population trans 0.43 Population gauche+ 0.57
K49	$\chi_1$ : -	$\chi_1$ : -	${}^3J(C\gamma C') = 3.57 \pm 0.03$		$\chi_1$ : -	0.29	
L51	$\chi_2$ : +	$\chi_2$ : N		$C(\delta_1), C(\delta_2) = 24.1$ ppm; $\Delta CS = 0$ ppm	$\chi_2$ : +	0.44	
	$\chi_1$ : +	$\chi_1$ : ?			$\chi_1$ : -		
	$\chi_2$ : +	$\chi_2$ : +			$\chi_2$ : +		

\*+, conformational heterogeneity observed in crystal structure; -, no conformational heterogeneity observed; a, anisotropic electron density observed; m, multiple rotamers observed among different apo SpA-domain structures.

<sup>†</sup>Dynamic side chains as detected by <sup>3</sup>J averaging and/or chemical shift deviations from static limits; +, dynamic  $\chi_1$  or  $\chi_2$ ; -, static  $\chi_1$  or  $\chi_2$ ; N, no observation; ?, ambiguous assignment.

<sup>‡</sup>Values close to 0 indicate low conformational heterogeneity; values close to 1 indicate high conformational heterogeneity (see text).

<sup>§</sup>Residues that make contact with F<sub>c</sub>.

**Table S4. Data collection and refinement statistics for SpA<sup>C</sup> Q9W**

SpA <sup>C</sup> Q9W	
Data collection	
Space group	<i>P6<sub>5</sub></i>
Cell dimensions	
<i>a</i> , <i>b</i> , <i>c</i> , Å	44.5, 44.5, 116.1
$\alpha$ , $\beta$ , $\gamma$ , °	90.0, 91.0, 120.0
Wavelength	1.0
Resolution, Å	50.00–1.87 (1.90–1.87)*
<i>R</i> <sub>sym</sub>	0.091 (0.72)
<i>I</i> / $\sigma$ <i>I</i>	123.5 (2.6)
Completeness, %	99.9 (100.0)
Redundancy	17.0 (10.5)
Refinement	
Resolution, Å	36.6–1.87
No. of reflections	9,603
<i>R</i> <sub>work</sub> / <i>R</i> <sub>free</sub>	19.9/25.6
No. of atoms	
Protein	921
Water	22
B factors	
Protein	59.3
Water	69.5
Rms deviations	
Bond lengths, Å	0.013
Bond angles, °	1.189

\*Data were collected from a single crystal. Values in parentheses are for the highest-resolution shell.

**Table S5. Data collection and refinement statistics for SpA<sup>C</sup> Q9W in complex with F<sub>c</sub>**

SpA <sup>C</sup> Q9W–F <sub>c</sub> complex	
Data collection	
Space group	<i>C2</i>
Cell dimensions	
<i>a</i> , <i>b</i> , <i>c</i> , Å	138.0, 87.2, 103.2
$\alpha$ , $\beta$ , $\gamma$ , °	90.0, 91.1, 90.0
Wavelength	1.0
Resolution, Å	50.00–2.28 (2.32–2.28)*
<i>R</i> <sub>sym</sub>	0.137 (1.0)
<i>I</i> / $\sigma$ <i>I</i>	19.9 (1.6)
Completeness, %	100.0 (99.8)
Redundancy	7.9 (6.2)
Refinement	
Resolution, Å	34.8–2.28
No. of reflections	52,860
<i>R</i> <sub>work</sub> / <i>R</i> <sub>free</sub>	19.6/24.2
No. of atoms	
Protein	6,197
Water	126
B factors	
Protein	61.91
Water	53.28
Rms deviations	
Bond lengths, Å	0.016
Bond angles, °	1.506

\*Data were collected from a single crystal. Values in parentheses are for the highest-resolution shell.